

# Noro-Frenkel scaling in short-range square well: A Potential Energy Landscape study

Giuseppe Foffi<sup>1,\*</sup> and Francesco Sciortino<sup>2,†</sup>

<sup>1</sup>*Institut Romand de Recherche Numérique en Physique des Matériaux IRRMA, PPH-Ecublens, CH-105 Lausanne, Suisse*

<sup>2</sup>*Dipartimento di Fisica and INFN-CNR-CRS Soft,  
Università di Roma La Sapienza, P.le A. Moro 2, 00185 Roma, Italy*

We study the statistical properties of the potential energy landscape of a system of particles interacting via a very short-range square-well potential (of depth  $-u_0$ ), as a function of the range of attraction  $\Delta$  to provide thermodynamic insights of the Noro and Frenkel [M.G. Noro and D. Frenkel, J.Chem.Phys. **113**, 2941 (2000)] scaling. We exactly evaluate the basin free energy and show that it can be separated into a *vibrational* ( $\Delta$ -dependent) and a *floppy* ( $\Delta$ -independent) component. We also show that the partition function is a function of  $\Delta e^{\beta u_0}$ , explaining the equivalence of the thermodynamics for systems characterized by the same second virial coefficient. An outcome of our approach is the possibility of counting the number of floppy modes (and their entropy).

PACS numbers: 61.20.Ja, 82.70.Dd, 82.70.Gg, 64.70.Pf

Colloid and protein systems are often characterized by interactions on a length scale significantly smaller than the particle size. When the interaction range is less than 10% of the repulsive diameter, both thermodynamic and dynamic properties are drastically different from the standard liquid behavior [1, 2, 3, 4, 5]. An important characteristic of short-range spherical potentials  $V(r)$  is the independence of thermodynamic properties by the specific  $V(r)$  shape. In particular, the reduced second virial coefficient  $B_2^* \equiv B_2/B_2^{HS} \equiv -2\pi \int (1 - e^{-\beta V(r)}) r^2 dr / B_2^{HS}$  (where  $B_2^{HS}$  is the hard-sphere  $B_2$ ) appears to be a proper scaling variable which combines temperature  $T$  and potential shape. Based on the analysis of several available theoretical and numerical data, Noro and Frenkel (NF) [6] have proposed a generalized law of corresponding states which states that all short-ranged spherically symmetric attractive potentials are characterized by the same thermodynamics properties if compared at the same reduced density and  $B_2^*$ . This universal behavior is captured by the extreme limit of vanishing interaction range, i.e. by the celebrated Baxter sticky sphere model [7], which, despite its known pathologies [8, 9] has been successfully used to interpret experimental results in colloidal and proteins systems. The available accurate estimates of the critical point location and two-phase coexistence of the Baxter model [10] are becoming the reference for the thermodynamic behavior of all short-range spherical potentials.

In this Letter we study the NF empirical scaling [6] in the potential energy landscape (PEL) thermodynamic framework, focusing on particles interacting via square-well (SW) potential of different well-width  $\Delta$ , to provide a deeper understanding of the generalized law of corresponding states. We first show that for this model the

NF-law holds in a large range of densities (not only close to the liquid-gas critical point) and correctly reproduce the Baxter behavior in the limit of vanishing  $\Delta$ . Then we calculate, with no approximations, the statistical properties of the PEL [11, 12, 13] and their dependence on the well width. This study allows us to separate the basin free entropy in two components, respectively reflecting the exploration of the bond volume ( $\Delta$ -dependent) and the exploration of the available volume at fixed bond distance ( $\Delta$ -independent). This second contribution is the only one existing in the Baxter model.

To generate equilibrated configurations, we perform event-driven molecular dynamics (EDMD) simulations [14] for the SW potential, defined by a potential well of depth  $u_0 = -1$  and well width  $\Delta$ . We investigate values of  $\Delta/d$  ranging from  $10^{-1}$  to  $10^{-3}$ , where  $d = 1$  is the hard-core particle diameter, chosen as unity of length. Pairs of particles are considered bonded when their relative distance is between  $d$  and  $d + \Delta$ . Density is expressed as packing fraction  $\phi = \frac{\pi}{6} \rho d^3$ , where  $\rho = N/L^3$ ,  $N$  being the number of particles and  $L$  the simulation box size. According to the NF law, the thermodynamic of the system is controlled by  $B_2^*$  and  $\phi$ , at least in the proximity of the critical point. In the SW case  $B_2^* - 1 \sim \Delta e^{u_0/T}$  in the limit of short well-width.

Fig. 1 shows the potential energy per particle  $U/N$  (panel a) and the compressibility factor  $Z = PV/Nk_B T$  (panel b) as a function of  $\phi$  for several  $\Delta$  values, at  $B_2^* = -0.40$ . For  $\Delta < 0.05$ , all curves collapse on the same curve confirming the validity of NF scaling also outside the critical region. Similar behavior is observed for other different  $B_2^*$  values. The value at which the scaling breaks, i.e.  $\Delta \sim 0.05$ , is in close agreement with the value at which the Baxter solution ceases to be a valid approximation for the SW model [15]. To confirm that the SW potential approaches the Baxter model in the limit of vanishing  $\Delta$  (and as a confirmation of our ability to equilibrate configurations at small  $\Delta$  values) we compare in Fig. 1c the recently calculated radial distribution function  $g(r)$

\*Electronic address: giuseppe.foffi@epfl.ch

†Electronic address: francesco.sciortino@phys.uniroma1.it

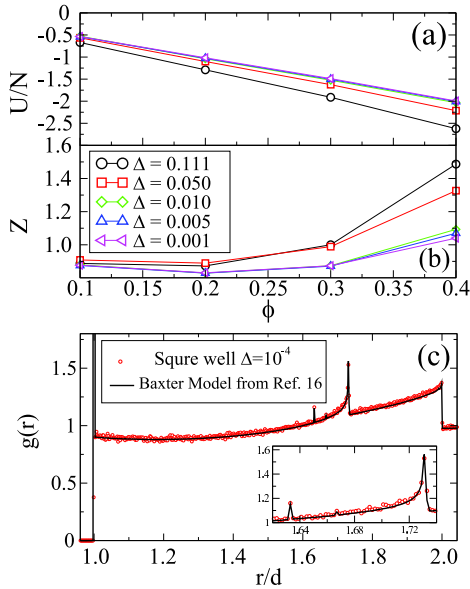


FIG. 1: (Color online) Top: (a) Energy per particle vs.  $\phi$  for various  $\Delta$  at  $B_2^* = -0.40$ . (b) same as (a) for compressibility factor  $Z = PV/Nk_B T$ . (c) Radial distribution function for  $\phi = 0.164$  and  $B_2^* = -0.92$ . The continuous line is from simulation of the Baxter model [16], dots are for a SW with  $\Delta = 10^{-4}$ .

of the Baxter model [10] with the the  $g(r)$  calculated for a SW system with  $\Delta = 10^{-4}$  at  $B_2^* = -0.92$ . The agreement between the two results is perfect. The shoulders and the  $\delta$ -functions indicating the presence of clusters with well defined structure [16] are reproduced both in their location and their height.

The fact that for  $\Delta < 0.05$  the state of the system is controlled by the values of  $\phi$  and of  $\Delta e^{\beta u_0}$ , suggests that — at fixed  $\phi$  — the configurational part of the partition function  $\mathcal{Z}$  must be, in leading order, a function of  $\Delta e^{\beta u_0}$ . In the PEL formalism [11, 12, 13] the phase space is decomposed into basins of attractions of the local minima of the PEL — the so-called inherent structures (IS) — and the partition function is written as a sum over all landscape basins, each of them weighted by the local minimum Boltzmann factor and by the basin free-energy. In the SW case, we associate an IS to a specific bonding pattern [17] (thus, the IS energy is expressed by the total number of bonds  $N_b$ ) and the basin free-energy to the logarithmic of the (multidimensional) volume  $\Omega$  which can be explored in configuration space without breaking or reforming bonds. In this respect, the conceptual operation of thinking  $\mathcal{Z}$  as a sum over all possible PEL basins is equivalent to expressing  $\mathcal{Z}$  as a sum over all possible bonding pattern [18]. Since the Boltzmann factor weighting the probability of each configuration is  $e^{\beta u_0 N_b}$ , scaling in the variable  $\Delta e^{\beta u_0}$  implies that the number of states  $\Omega$  sampled by each fixed bonding pattern must scale with  $\Delta$  as  $\Delta^{N_b}$ , i.e. each bond is independent and contributes a quantity of order  $\Delta$  to  $\Omega$ . This is the hypothesis that we test next.

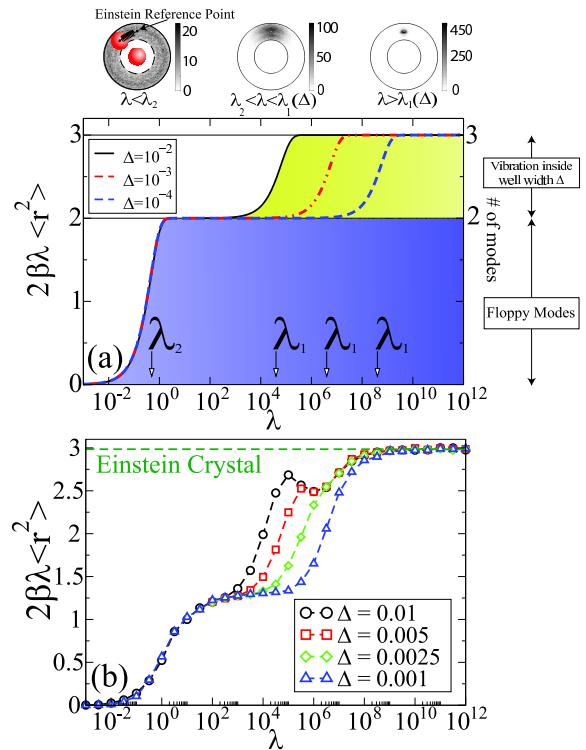


FIG. 2: (Color online) Top: Mean square displacement of a particle harmonically bounded to a reference point and interacting via a SW with a particle located in the origin for different  $\lambda$  values. The probability distribution of the particle is schematically shown above the plot for three representative values of  $\lambda$ : particle completely delocalized (left), particle localized by the bond (center) and particle localized by the harmonic force (right).  $\lambda_1$  and  $\lambda_2$  are discussed in the text. Bottom: Mean square displacement  $2\beta\lambda\langle\sum_i(\mathbf{r}_i - \bar{\mathbf{r}}_i)^2\rangle_\lambda/N$  (labelled  $2\beta\lambda\langle r^2 \rangle$  for semplicity in the figure) for a SW system with  $\phi = 0.30$  and  $B_2^* = -0.69$  vs.  $\lambda$ , for different  $\Delta$  values. The Einstein limit is shown as a dashed line.

To precisely estimate  $\Omega$  we implement a generalization of the thermodynamic integration technique first used by Ladd and Frenkel to evaluate the free energy of the hard sphere crystals [19]. In this technique, the system Hamiltonian  $H_0$  is complemented by an harmonic term  $\lambda \sum_i (\mathbf{r}_i - \bar{\mathbf{r}}_i)^2$  centered around a reference configuration  $(\bar{\mathbf{r}}_1, \dots, \bar{\mathbf{r}}_N)$  of strength  $\lambda$  acting on each particle. The essence of this method lies in the possibility of performing a thermodynamic integration over  $\lambda$  from a state of known free energy to the state of interest ( $\lambda = 0$ ). When  $\lambda$  is very large, particles harmonically oscillate around the reference state and the system behaves like a collection of  $3N$  harmonic oscillators, i.e. an Einstein solid. If the unperturbed system is identified with a specific bonding pattern and  $H_0$  is defined as zero if the configuration has the correct bonding pattern and infinity if the bonding pattern has changed (i.e. if a bond is broken or a new bond is formed), then the result of the thermodynamic integration provides an exact measure of the basin free

energy. Since the exploration of space within the fixed bond-pattern basin takes place on a flat energy surface the only contribution to the basin free energy is entropic. The basin entropy per particle in units of  $k_B$ ,  $\sigma_{\text{basin}}$ , can be formally written as [18]

$$\sigma_{\text{basin}} = -\beta f_E(T, \lambda_\infty) + \int_0^{\lambda_\infty} \lambda \langle \sum_i (\mathbf{r}_i - \bar{\mathbf{r}}_i)^2 \rangle_\lambda d \ln \lambda \quad (1)$$

where  $f_E(T, \lambda)$  is the free energy of  $3N$  harmonic oscillators coupled by an elastic constant  $\lambda$ ,  $\langle \cdot \rangle_\lambda$  an ensemble average at a fixed value of  $\lambda$  and  $\lambda_\infty$  is any value of  $\lambda$  such that the harmonic contribution is dominant as compared to  $H_o$  and thus  $\langle \lambda \sum_i (\mathbf{r}_i - \bar{\mathbf{r}}_i)^2 \rangle_\lambda \approx \frac{3}{2} N k_B T$ . From a technical point of view we evaluate  $\langle \lambda \sum_i (\mathbf{r}_i - \bar{\mathbf{r}}_i)^2 \rangle_\lambda$  for thirty or more  $\lambda$  values between  $\lambda_\infty$  and 0 via MC simulations rejecting all moves which modify the bond-pattern.

To guide the interpretation of the numerical results it is helpful to examine the behavior of two particles bonded by a square-well in three dimensions. Fixing particle 1 at the origin (to neglect the trivial center of mass degrees of freedom) and selecting an Einstein reference site acting on particle 2 in an arbitrary position  $\bar{\mathbf{r}}_2 \equiv (x, 0, 0)$  (with  $d < x < d + \Delta$ ), the resulting  $\langle (\mathbf{r}_2 - \bar{\mathbf{r}}_2)^2 \rangle_\lambda$  is

$$\lambda \langle (\mathbf{r}_2 - \bar{\mathbf{r}}_2)^2 \rangle_\lambda = -\frac{\partial}{\partial \beta} \log \mathcal{Z}_\lambda(\beta), \quad (2)$$

where the generating (or partition) function  $\mathcal{Z}_\lambda(\beta)$  is

$$\mathcal{Z}_\lambda(\beta) = 2\pi \int_d^{d+\Delta} \frac{e^{-\beta\lambda(r+x)^2} (e^{-4\beta\lambda rx} - 1)}{2\beta\lambda} r dr \quad (3)$$

The resulting  $\lambda$  dependence of  $2\beta\lambda \langle (\mathbf{r}_2 - \bar{\mathbf{r}}_2)^2 \rangle_\lambda$  is shown in Fig. 2a for three different values of  $\Delta$ . At large  $\lambda$  (the harmonic limit), the quantity  $2\beta\lambda \langle (\mathbf{r}_2 - \bar{\mathbf{r}}_2)^2 \rangle_\lambda$  goes to three, the total number of degrees of freedom. On decreasing  $\lambda$ , the function shows a two-step decay to zero with an intermediate plateau at the value two. The two cross-overs (from 3  $\rightarrow$  2 and from 2  $\rightarrow$  0) are taking place at values of  $\lambda_1 \approx (2/\Delta)^2$  and  $\lambda_2 \approx (2/d)^2$ . To interpret this behavior we recall that for very large  $\lambda$  ( $\lambda > \lambda_1$ ) confinement is provided by the harmonic potential. For  $\lambda_2 < \lambda < \lambda_1$ , confinement of the harmonic potential has become larger than  $\Delta$  and the bond distance becomes the relevant quantity controlling the mean square displacement. For even smaller  $\lambda$  ( $\lambda < \lambda_2$ ) confinement is provided by the finite bond volume (a corona of width  $\Delta$  and inner surface  $4\pi d^2$ ). The two-step cross-over makes it possible to count the number of modes which are related to exploration of the bond width and the number of modes which are related to exploration of space at fixed interparticle distance. Indeed, the first cross-over is  $\Delta$ -dependent while the second one is  $\Delta$ -independent. Hence, the FL method allows one not only to evaluate the total change in entropy but also to count (and separate !) the number of modes which are related to

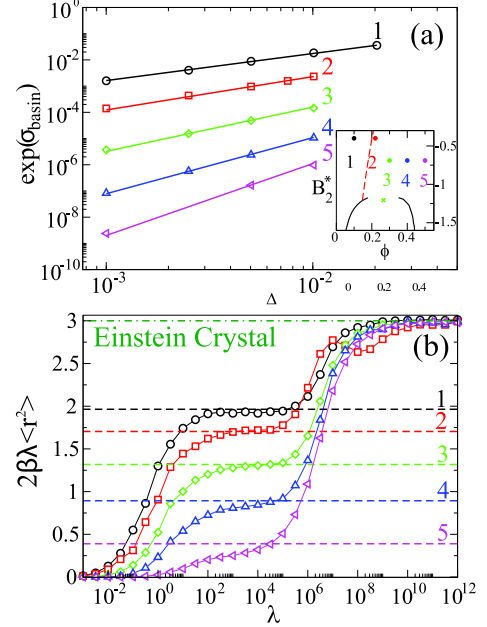


FIG. 3: (Color online) Top: Number of state sampled  $\Omega^{1/N} = \exp(\sigma_{\text{basin}})$  vs.  $\Delta$  for different state points. The straight lines are single parameter fit of the form  $A\Delta^{n_b}$  where  $n_b$  is the number of bonds per particle per particle, i.e.  $n_b = N_b/N$ . The inset shows the the location of the corresponding state points in the  $B_2^*$  -  $\phi$  phase diagram. It also show the percolation line (dashed line) and the liquid-gas coexistence from Ref.10 Bottom: Symbols are  $2\beta\lambda \langle \sum_i (\mathbf{r}_i - \bar{\mathbf{r}}_i)^2 \rangle_\lambda / N$  (labelled  $2\beta\lambda \langle r^2 \rangle$  for semplicity in the figure) vs.  $\lambda$  for  $\Delta = 10^{-3}$ ; The dashed horizontal line are  $3 - n_b$ . Note that the intermediate  $\lambda$  plateau is well reproduced by the fraction of floppy modes  $f_f = 3 - n_b$ .

the exploration of the bond-distance (vibrational modes) from the modes which are related to the exploration of the volume with rigid bonds (floppy modes). The behaviour of  $2\beta\lambda \langle \sum_i (\mathbf{r}_i - \bar{\mathbf{r}}_i)^2 \rangle_\lambda / N$  for a bond configuration of 200 particles (a typical equilibrium configuration produced by MD simulation) for different values of  $\Delta$  is shown in Fig. 2b. The bonding network is identical for all  $\Delta$  values. As in the two-particles example, the shape of the curve shows two parts, one  $\Delta$ -independent and one  $\Delta$ -dependent. As from Eq. 1, the area under the  $\lambda \langle \sum_i (\mathbf{r}_i - \bar{\mathbf{r}}_i)^2 \rangle_\lambda / N$  vs  $\ln \lambda$  curve is a measure of  $\sigma_{\text{basin}}$ , the entropy associated to the exploration of space at fixed bonding pattern. The  $\Delta$ -independent and the  $\Delta$ -dependent parts of  $\lambda \langle \sum_i (\mathbf{r}_i - \bar{\mathbf{r}}_i)^2 \rangle_\lambda$  give rise to two different contribution to  $\sigma_{\text{basin}}$ , which we can identify as the floppy [20]  $\Delta$ -independent — the dark shaded region in the cartoon in Fig. 2a — ( $N\sigma_{\text{floppy}} = \ln \Omega_{\text{floppy}}$ ) and the vibrational  $\Delta$ -dependent part — the light coloured region — ( $N\sigma_{\text{vib}} = \ln \Omega_{\text{vib}}$ ).

According to the PEL picture of the NF law,  $\Omega_{\text{basin}}^{1/N} = e^{\sigma_{\text{basin}}}$  must be proportional to  $\Delta^{n_b}$ , where  $n_b \equiv N_b/N$  is the number of bonds per particle. This prediction can be put under severe test, since both  $\Delta$  and  $n_b$  are

a-priori known, by comparing the calculated values for  $e^{\sigma_{\text{basin}}}$  with  $\Delta^{n_b}$ . This comparison is reported in Fig. 3a for several typical bonding configurations with different bonding patterns, extracted from equilibrium simulations at different  $\phi$  and  $T$ , encompassing the range  $1.03 < n_b < 2.61$ . In all studied cases,  $\Omega_{\text{basin}} \sim \Delta^{n_b}$  with extreme accuracy. The validity of such relationship suggests that for short-range SW, each bond acts as an independent unit (so that the vibrational entropy of the bonding pattern coincides with the sum of all the bond entropies). In the PEL language, the NF scaling is an expression of the independence of the bonds. In this respect, proper scaling between different potential shapes is predicted when the vibrational free energy of a bonded pair is chosen as a proper scaling variable. The possibil-

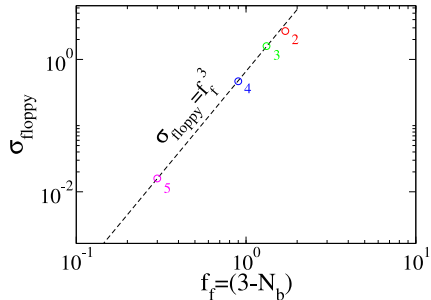


FIG. 4: (Color online) Entropy of the floppy modes ( $\sigma_{\text{floppy}}$ ) vs fraction of floppy modes ( $f_f = 3 - N_b/N$ ). The straight line is a power law with exponent 3, i.e.  $\sigma_{\text{floppy}} \propto f_f^3$ .

ity of separating in a precise way  $\Omega_{\text{vib}}$  and  $\Omega_{\text{floppy}}$  (see the cartoon in Fig. 2a), allows us to evaluate also the ( $\Delta$ -independent) volume in configuration space sampled by the a specific bonding pattern when all bond distances are fixed. This volume corresponds to the free rolling motions of the particles with no bond-breaking of -forming and it is essentially the basin volume accessible to the

Baxter model. It is interesting to investigate the dependence of this quantity on the number of bonds, since one expect that on increasing the connectivity, the entropy of the floppy modes should decrease. For the short-range SW under consideration the fraction of floppy modes (the height of the plateau in  $2\beta\lambda\langle\sum_i(\mathbf{r}_i - \bar{\mathbf{r}}_i)^2\rangle_\lambda/N$ ) is found to be  $f_f = 3 - n_b$  (see Fig. 3b), a value consistent with the existence of  $N_b$  independent vibrational degrees of freedom. Hence, the total floppy entropy (the area under the curve – see Eq. 1) should vanish close to the point when  $n_b \approx 3$  (i.e. each particle is involved in average in six bonds). This expectation is indeed born out in the calculated  $f_f$ -dependence of  $\sigma_{\text{floppy}}$  shown in Fig. 4. Unexpectedly, the floppy entropy goes to zero as a power law  $\sigma_{\text{floppy}} \propto f_f^3$ . The value of the exponent suggests that not only the number of modes but also the floppy entropy per mode vanishes with a power-law close to  $f_f = 0$ . It is interesting to observe that at the state point where  $N_b \approx 3N$ , the full entropy of the system would be given only by the logarithm of the number of topologically different bonding patterns.

In conclusion, we have shown that the empirical NF-law of corresponding states can be explained in the rigorous PEL thermodynamic formalism as arising from the additive contribution of the bonds to the basin entropy. An unexpected outcome of this study is a new methodology to separately evaluate the fraction of floppy modes and their entropy for any specific bonded configuration, a method which can be used in studies of the rigidity of hard particle systems [21].

We thank D. Frenkel, M. Miller and R. Sear for useful discussions. We also thank M. Miller for providing us the Baxter  $g(r)$  data and C. De Michele for the EDMD code. We acknowledge support from the Swiss National Science Foundation (Grant No. 99200021-105382/1) (G.F.), from MIUR-FIRB and Cofin (F.S.) and from Training Network of the Marie-Curie Programme of the EU (MRT-CT-2003-504712).

---

[1] V. Anderson and H. Lekkerkerker, *Nature* **416**, 811 (2002).  
[2] V. Trappe and P. Sandkühler, *Curr. Opin. Colloid Int. Sci.* **8**, 494 (2004).  
[3] K. A. Dawson et al., *Phys. Rev. E* **63**, 11401 (2001).  
[4] K. N. Pham et al., *Science* **296**, 104 (2002).  
[5] F. Sciortino and P. Tartaglia, *Advances in Physics* **54**, 471 (2005).  
[6] M. Noro and D. Frenkel, *J. Chem. Phys.* **113**, 2941 (2000).  
[7] R. J. Baxter, *J. Chem. Phys.* **49**, 2770 (1968).  
[8] G. Stell, *J. Stat. Phys.* **63**, 1203 (1991).  
[9] S. Fishman and M. Fisher, *Physica A* **108**, 1 (1981).  
[10] M. A. Miller and D. Frenkel, *Phys. Rev. Lett.* **90**, 135702 (2003).  
[11] F. Stillinger and T. Weber, *Science* **225**, 983 (1984).  
[12] D. Wales, *Energy Landscapes : Applications to Clusters, Biomolecules and Glasses* (Cambridge University Press, 2003).  
[13] F. Sciortino, *J. Stat. Mech.* p. P05015 (2005).  
[14] D. C. Rapaport, *The Art of Molecular Dynamic Simulation* (Cambridge University Press, 1995).  
[15] A. Malijevsky et al., *J. Chem. Phys.* **125**, 074507 (2006).  
[16] M. A. Miller and D. Frenkel, *J. Phys.: Condens. Matter* **16**, S4901 (2004).  
[17] Note that our definition of IS does not require a minimization procedure. Two configurations related by a path of decreasing energy (i.e. which can be connected by moves which requires or zero or a negative change of energy) are considered belonging to distinct basins.  
[18] A. J. Moreno et al., *Physical review letters*. **95**, 157802 (2005).  
[19] D. Frenkel and B. Smit, *Understanding Molecular Simulation* (Academic Press, London, 2001), 2nd ed.  
[20] G. Naumis, *Physical Review E - Statistical, Nonlinear,*

and Soft Matter Physics **71**, 026114/1 (2005).  
[21] M. Thorpe and P. Duxbury, eds., *Rigidity Theory and Applications* (Springer, 1999).